

Supporting Information

Electronic phase-crossover and room temperature ferromagnetism in a two-dimensional (2D) spin lattice

A. K. Nair¹, S. J. Ray^{1*}

¹Department of Physics, Indian Institute of Technology Patna,
Bihta 801106, India

* Email: ray@iitp.ac.in

Results and Discussion

S1. Total energy difference ($E_{\text{FM}} - E_{\text{AFM}}$) of various magnetic arrangements with strain

The energies of all the magnetic configurations which include 1 ferromagnetic (FM) and 3 antiferromagnetic (AFM) configurations denoted by AFM1, AFM2 and AFM3 are calculated. The energies of these configurations at different values of strain are listed in Table S1.

Table S1: Total energies for various magnetic configuration and energy difference (FM-AFM) calculated for different strains.

Strain (%)	FM (eV)	AFM (eV)			$E_{\text{FM}} - E_{\text{AFM}}$ (meV)
		AFM1	AFM2	AFM3	
0	-18320.95340	-18320.38796	-18320.90322	-18320.58265	-50.18
2	-18320.91050	-18320.23064	-18320.78708	-18320.48860	-123.42
4	-18318.35911	-18317.59076	-18318.16625	-18317.90926	-192.86
6	-18314.96475	-18314.16879	-18314.70499	-18314.51406	-259.76
8	-18311.72145	-18310.98389	-18311.43760	-18311.30349	-283.85
10	-18308.93011	-18308.29700	-18308.65398	-18308.57515	-276.16
12	-18306.65726	-18306.10643	-18306.42509	-18306.38489	-232.17
14	-18304.86995	-18304.36670	-18304.66569	-18304.65144	-204.26
16	-18303.42447	-18303.03531	-18303.29925	-18303.31523	-109.24
18	-18302.39424	-18302.03796	-18302.15260	-18302.31302	-81.22
20	-18301.62890	-18301.27704	-18301.41791	-18301.54930	-79.60

From the above table it can be observed that, for the strain range -1% to 14%, AFM2 is offers lowest energy while AFM3 stays with minimum energy between the strain range of 16% to 20% between various AFM configurations.

S2. Phonon calculations of the strained structures

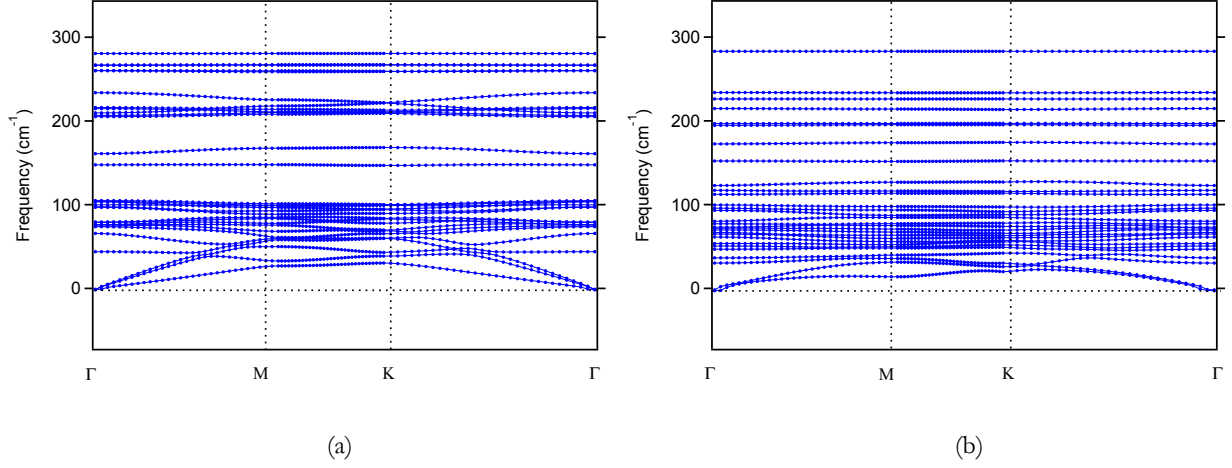


Figure S1: Phonon bandstructures plotted for strain cases applied along biaxial direction with magnitude: (a) unstrained (b) $S_b = +8\%$

The phonon bandstructures provides insights into the structural stability of the system at various strain rates as illustrated in the above figures. The $1 \times 1 \times 1$ unit cell consisting of 2 atoms each of Cr, Ge, and 6 atoms of Te were considered for the phonon dispersion calculations. The k-point mesh of $4 \times 4 \times 1$ was taken into account, while also enabling the finite displacement method, and a phonon convergence threshold of 1×10^{-14} eV was set for better accuracy.

From the above figure, it can be noted that there is no occurrence of negative phonon frequencies in the unstrained condition. Also, the same holds true in the case of the strained system at $S_b = +8\%$ as well. Therefore, this interpretation reveals that the material is stable at this high strain condition. The phonon bands also start and end at the Γ (zone center). The absence of imaginary bands in the above two cases indicate the stability of the structure under different strain conditions.

S3. Exfoliation energy of $\text{Cr}_2\text{Ge}_2\text{Te}_6$

Exfoliation energy is an important parameter to be considered while fabricating 2D structures. Exfoliation energy of n-layer CGT ($E_{exf}(n)$) is calculated using the equation below:

$$E_{exf}(n) = \frac{E_{iso}(n) - E_{bulk}(n/m)}{A}$$

Where $E_{iso}(n)$ is the total energy of the unit cell of isolated n-layer CGT in vacuum while E_{bulk} is the total energy of the unit cell of bulk CGT possessing m layers (i.e. $m = 3$ for a trilayer $\text{Cr}_2\text{Ge}_2\text{Te}_6$), E_{bulk}/m represents the energy of the bulk material per layer and A is the in-plane surface area of the bulk unit cell of CGT. The results are represented in the form of a table shown below.

Table S2: Table representing the exfoliation energy of n-layer Cr₂Ge₂Te₆

Layers (n)	Exfoliation energy (meV/Å ²)
2	10.0196
3	13.3474
4	15.0498
5	16.1496
6	16.7280

As seen from the Table S2, the exfoliation energies of CGT fall in the range of 10-17 meV/Å² which is comparatively lower than the exfoliation energy of graphite which has a n-layer exfoliation energy in the range 21-24 meV/Å² (**Energy Storage Materials 25 (2020): 866-875, Nano letters 18, 5 (2018): 2759-2765**).

S4. Molecular dynamics (MD) simulations at various temperatures

Molecular dynamics (MD) simulations were performed on the unit cell of Cr₂Ge₂Te₆ at 500 K, 600 K and 700 K using the NVE ensemble (microcanonical ensemble) with the velocity-verlet integration algorithm. The simulation was run over 3×10^5 steps over a total simulation time of 300 ps.

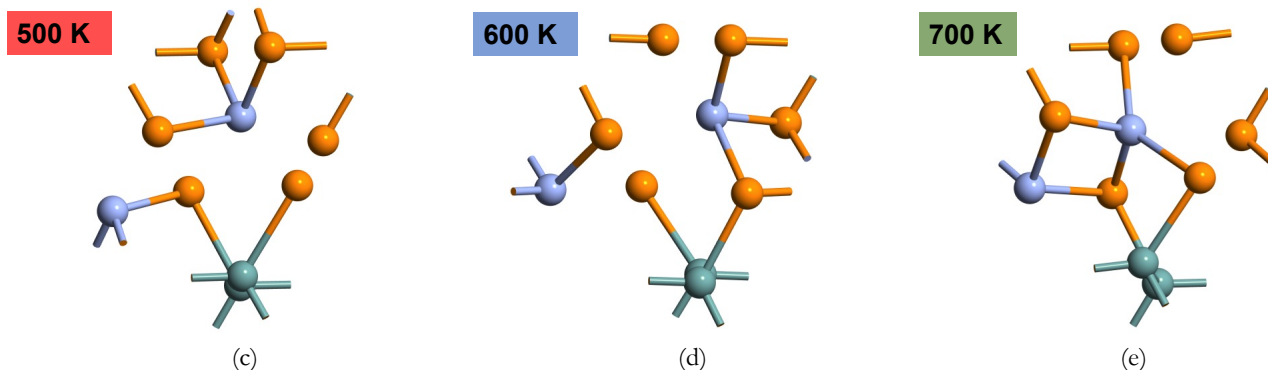
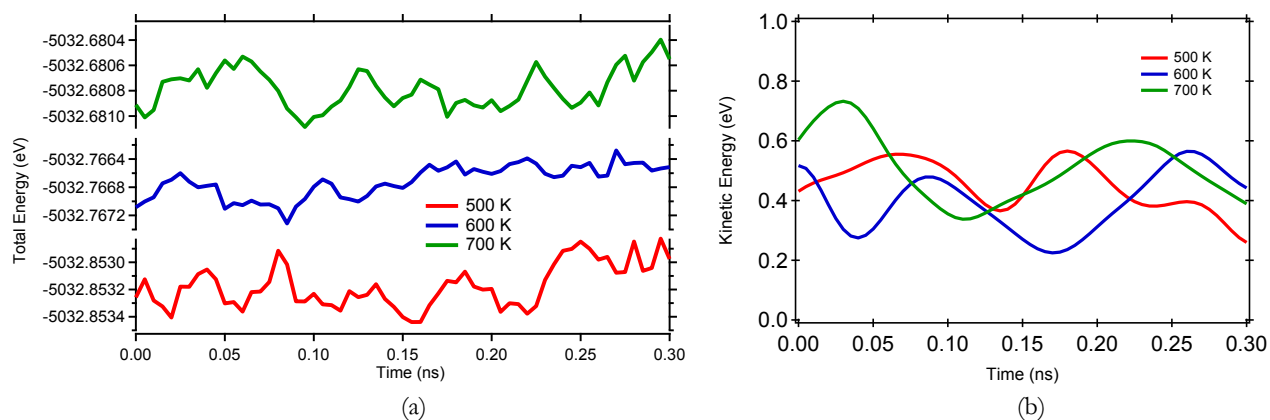


Figure S2: (a) Total energy of monolayer CGT as a function of time, (b) Variation in kinetic energy of the system with time. The final MD simulation images obtained for temperatures of (c) 500 K, (d) 600 K and (e) 700 K.

The MD simulation snapshots for each temperature depicted in Figs. S2 (c), (d) and (e) indicates that the system is thermally and dynamically stable. Also, from the total energy versus the time scale graph shown in Fig. S2 (a), it can be noticed that the difference in the total energy variations from 500 K to 700 K is ~ 0.17 meV which is a negligibly small, hence the reason for observing very minor displacements in atomic positions of CGT for the variation in temperature. The similar observations can also be noted in the kinetic energy as a function of time scale displayed in Fig. S2 (b). Experimental studies with CGT have reported measurements upto a high temperature of 1000 K, which also suggests high temperature structural stability of it, supporting our observation.

S5. Spin-orbit coupled (SOC) GGA calculation

Electronic bandstructure calculations were performed on unstrained CGT taking into account the spin-orbit coupling of the material.

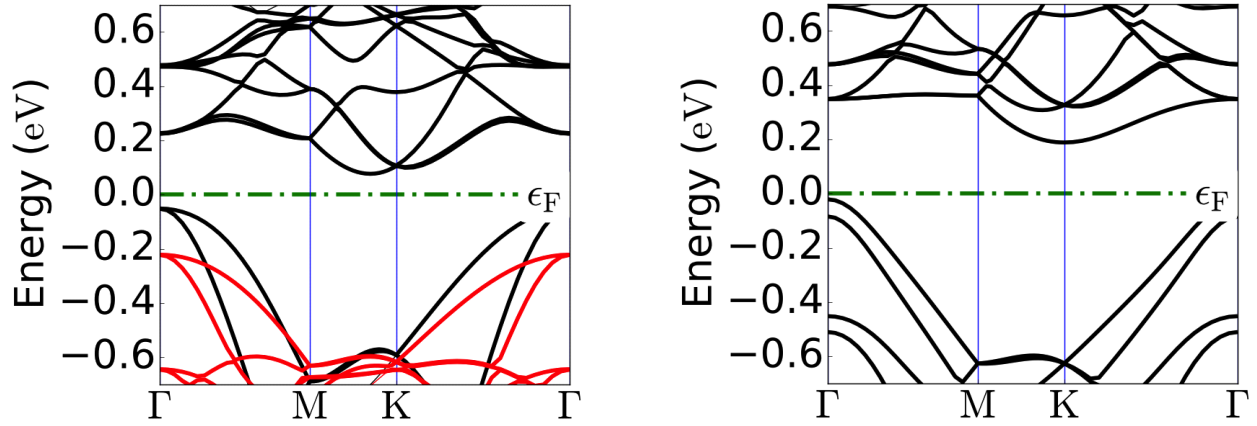


Figure S3: Bandstructure of pristine $\text{Cr}_2\text{Ge}_2\text{Te}_6$ considering (a) without SOC, and (b) with SOC

S6. Magneto-anisotropic energy

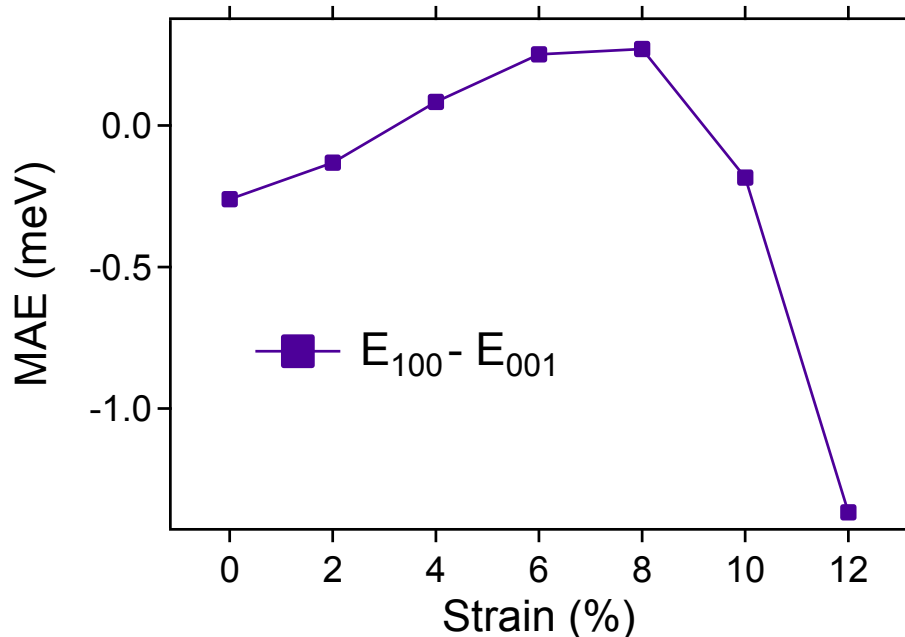


Figure S4: Magneto-anisotropic energy (MAE) difference for monolayer $\text{Cr}_2\text{Ge}_2\text{Te}_6$ as a function of strain along the in-plane (100) and out of plane (001) crystallographic directions.

The magneto-anisotropy energy for different strain percentages has been calculated and is depicted in Fig. S4. It was observed that both the in-plane crystallographic directions i.e. $\{100\}$ and $\{010\}$ are equally preferred by the spins for different values of strain. The spins prefer to stay in-plane in the unstrained condition which is also the case at most strain cases.

S7. Projected density of states (PDOS) analysis for understanding the electric field effect on $\text{Cr}_2\text{Ge}_2\text{Te}_6$

Projected density of states (PDOS) analysis is performed to understand the changes noticed in the strained ($S_b = +8\%$) structure of CGT on exposing the system to an electric field of $1 \text{ V}/\text{\AA}$ as shown in Fig.S5. The superexchange between the magnetic Cr atoms is mediated via the Te atoms and the major contributing orbitals towards this interaction are the $d_{xz}/d_{x^2-y^2}$ of Cr and $p_x/p_y/p_z$ of Te atoms. On exposing the strained ($S_b = +8\%$) structure of CGT to an electric field of $1 \text{ V}/\text{\AA}$, changes in the orbital contributions of the mediator Te atoms near the Fermi level is observed as portrayed in the PDOS (Fig. S5(b)) in comparison to the Fermi level orbital contributions when no electric field is applied on the system as shown in Fig.S5(a). Also, when the strained system ($S_b = +8\%$) is exposed to an electric field of $1 \text{ V}/\text{\AA}$, there is slight increase in the orbital contribution near the Fermi level (Fig. S5(b)) causing an eventual increase in the critical temperature to 331 K, which is also confirmed from the total energy difference of the two magnetic states (FM and AFM).

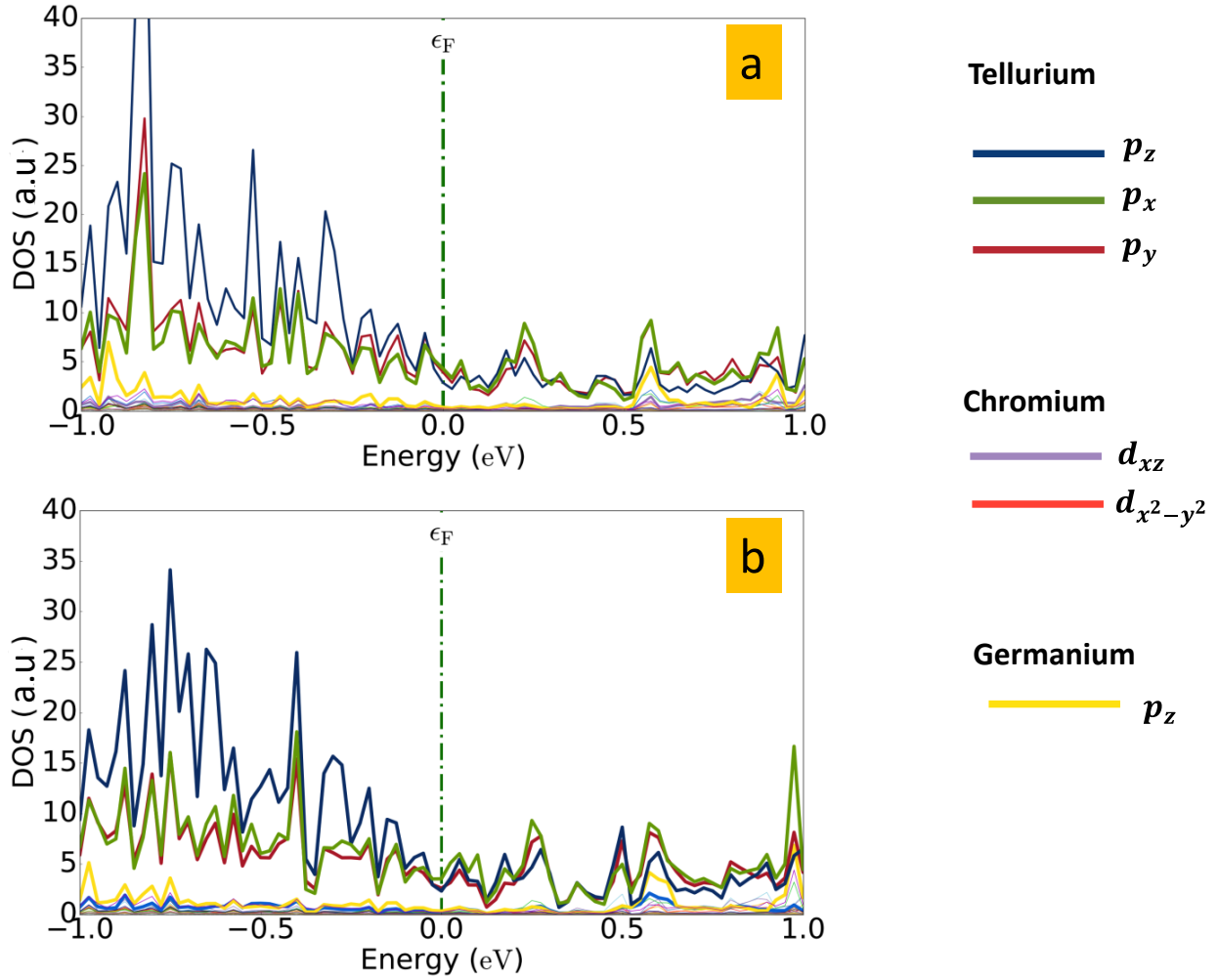


Figure S5: The projected density of states (PDOS) of strained ($S_b = +8\%$) configuration of CGT on the application of an electric field of (a) 0 V/Å and (b) 1 V/Å.